Theory of photoinduced structure changes

Naoto Nagaosa and Tetsuo Ogawa
Department of Applied Physics, Faculty of Engineering, The University of Tokyo, 7-3-1 Hongo, Bunkyo-ku, Tokyo 113, Japan
(Received 9 December 1987; revised manuscript received 21 September 1988)

A unified theory is presented to understand the dynamical properties of photoinduced structure changes, investigating mainly switching phenomena. The way *local microscopic* structure changes induced by optical pumping lead cooperatively to *global macroscopic* changes is clarified. Both the optical and thermal transitions are discussed, stressing their respective roles and qualitative differences. The dynamics of the system is described by the *kinetic Ising model* with rather complicated transition probabilities. When the three-dimensional interaction is large enough and the energy difference between the two states is small, the nucleation process can be neglected. We apply the *mean-field approximation* to the kinetic Ising model, and the dynamics, including threshold behavior, the relaxation time, and the spontaneous emission are discussed for low temperatures compared with the lattice relaxation energy. A strong temperature dependence of the dynamics is predicted. As an application of our theory, the photoisomerization (*A-B* transition) of polydiacetylenes is discussed to point out their collective nature.

I. INTRODUCTION

Structural changes as a result of relaxation after optical pumping have been studied extensively in the fields of photochemistry and solid-state optics. The investigations thus far, however, have mainly studied the detailed *microscopic* mechanisms of the *local* reactions or structure changes. The *macroscopic* structure changes are only vaguely understood as the simple summation of the local reactions. In condensed matter, particularly in solids, the interaction between local structure changes brings about the nonlinearity and can give rise to a new cooperative phenomenon which is absent in the dilute phase. One of the most promising candidates for this kind of phenomenon is photoinduced switching between the two macroscopically distinct states, which is also important to their potential applications to erasable photomemory systems. Photochromism,[1] photochemical hole burning,[2] photopolymerization,[3,4] and photoisomerization[5–11] are examples of the above phenomenon. Experimentally, it is also found that these phenomena are sensitive to the temperature, and the thermal processes as well as the optical ones play essential roles in the structure changes. In this paper we present a unified theory to understand the static and dynamical properties of this photoinduced switching phenomenon clarifying the respective role of optical and thermal processes.

We investigate a simple model which consists of the localized electronic two levels $|e_l\rangle$ and $|g_l\rangle$ at every site l with the Franck-Condon energy $E_{\rm FC}$. The excited state $|e_l\rangle$ is coupled with the interaction mode Q_l at site l with the lattice relaxation energy S. The interaction modes at sites l and l' are coupled with the coupling constant $K_{ll'}$, which brings about the collective nature.

Because the relaxation of the interaction mode Q_l is very rapid (within the time of order picosecond), it is reasonable to assume that Q_l is always in equilibrium with the given electronic state $|e_l\rangle$ or $|g_l\rangle$. After integrating out Q_l's, the model is reduced to the Ising model, where spin-up and spin-down states correspond to $|e_l\rangle$ and $|g_l\rangle$, respectively. The properties of the system in thermal equilibrium are, therefore, already known, as will be summarized in Sec. II. To discuss the nonequilibrium dynamics of the system, on the other hand, the transition rates between the two electronic states $|e_l\rangle$ and $|g_l\rangle$ should also be specified. These transition rates are composed of two contributions, i.e., optical and thermal transitions, in the model of the photoinduced structure changes. These two transitions are different qualitatively. The optical transitions occur vertically with respect to the interaction mode Q_l (Franck-Condon principle), while the thermal transition rates are governed by the potential barrier height between the two states. As a result, these two transitions play distinctive roles during the processes of the photoinduced structure changes. In summary, the model of the photoinduced structure changes is reduced to the kinetic Ising model with rather complicated transition rates with the external optical pumping. The energy difference between the two states corresponds to the magnetic field, and one state is absolutely stable while the other state is metastable.

Due to the theory of the nucleation process, the initial metastable state decays to the absolutely stable state with the creation of the critical droplet. The nucleation rate is determined by the creation energy of the critical droplet, and is quite different between one- and higher-dimensional systems. Previously we studied the linear chain model, where the nucleation process dominates, bearing the photopolymerization of diacetylene and diolefin crystals and photoisomerization of polydiacetylene crystals in mind.[12–14] We investigated the stability of a cluster of excited molecules with size m, and discussed the dynamical properties of the structure changes qualitatively based on it. In that model, there is no

"phase transition" in the thermodynamical sense because of the one dimensionality, and the interactions between the excited clusters were not taken into account.

When the three-dimensional interactions are taken into account, on the other hand, the critical droplet becomes large and the nucleation rate is very small if the energy difference between the two states is small. In this case, we can neglect the nucleation process within the time scale we are interested in, and the phase-transition-like threshold behavior can be expected. Recent experiments on the *A-B* transition in polydiacetylenes (PDA's) revealed the threshold behavior of the transformation rate as a function of the intensity of the incident light. In this paper we investigate the latter case, i.e., the switching phenomenon with the threshold behavior, as a nonequilibrium phase transition. Because the fluctuation, i.e., the nucleation process, is small, we propose the mean-field picture of this phenomenon. We treat the intersite couplings between relevant coordinates in the mean-field approximation, and the problem is reduced to that of the single site. The following points are discussed.

(1) The respective role of the optical and thermal transitions in the dynamics of the structure changes and their temperature dependence.

(2) The condition of the macroscopic structure change for the intensity of the optical pumping I_0 and its duration time t_0.

(3) The time required to reach the final relaxed state after the optical pumping is switched off.

(4) The comparison between the two directions of the switching.

According to the above items, the photoinduced switching is classified in the plane of $K(\equiv \sum_{l'} K_{ll'})$ and $\tilde{S}(\equiv S/E_{\rm FC})$, and we discuss the photoisomerization (*A-B* transition) of polydiacetylene crystals from this point of view.

In Sec. II the model is introduced and its connection to the kinetic Ising model and PDA's is clarified. The thermal equilibrium and the optical and thermal transitions are discussed there. Section III is devoted to the studies of the dynamics of the photoinduced structure changes in the mean-field approximation. Discussion, including the application to the polydiacetylene, and the conclusions are given in Sec. IV.

II. HAMILTONIAN AND THE KINETIC ISING MODEL

A. Hamiltonian

The switching phenomena recently found in polydiacetylenes, etc., are the result of the accumulation of the change in the electronic state and the configuration of the respective molecule due to the optical and/or the thermal transitions. Therefore we take two electronic states, i.e., the ground state $|g_l\rangle$ and the excited state $|e_l\rangle$, for the molecule at lth site. For example, in the case of the *A-B* transition of the polydiacetylenes, the electronic state of the molecule in the *B* phase corresponds to $|g_l\rangle$ while that in the *A* phase corresponds to $|e_l\rangle$. We start with the following Hamiltonian to describe the system:[12–14]

$$\mathcal{H}=\sum_l |e_l\rangle(E_{\rm FC}-\sqrt{S}\,Q_l)\langle e_l| +\tfrac{1}{2}\sum_l Q_l^2-\tfrac{1}{2}\sum_{l,l'} K_{ll'}Q_lQ_{l'} \tag{2.1}$$

and

$$|g_l\rangle\langle g_l|+|e_l\rangle\langle e_l|=1\ , \tag{2.2}$$

where $E_{\rm FC}$ is the Franck-Condon excitation energy, Q_l the relevant displacement which we treat as the classical variable, and $\sqrt{S}\,Q_l$ the Stokes shift in the $|e_l\rangle$ state at the lth molecule. The coupling constant between the displacements of the lth and l'th molecules is denoted as $K_{ll'}$, and its diagonal element K_{ll} is zero.

The relaxation of Q_l to the thermal equilibrium in each parabola finishes within the time of an order 10^{-13} sec (the inverse of the Debye frequency). Therefore we do not discuss this fast process in this paper, and assume that Q_l is always distributed around the bottom of one of the parabolas with the distribution functions P's given below:

$$P_g(Q_l)=\frac{1}{(2\pi k_BT)^{1/2}}\exp\left[-\frac{(Q_l-\Delta_l)^2}{2k_BT}\right], \tag{2.3a}$$

$$P_e(Q_l)=\frac{1}{(2\pi k_BT)^{1/2}}\exp\left[-\frac{(Q_l-\Delta_l-\sqrt{S}\,)^2}{2k_BT}\right], \tag{2.3b}$$

where k_B is the Boltzmann constant, T is the temperature, and Δ_l is defined by

$$\Delta_l=\sum_{l'\neq l} K_{ll'}Q_{l'}\ . \tag{2.4}$$

To integrate out the interaction modes Q_l's, we consider the partition function Z of the model Eq. (2.1):

$$Z={\rm Tr}_{\{\sigma\}}\int \mathcal{D}Q\exp\left[-\frac{\mathcal{H}(\{\sigma\},\{Q\})}{k_BT}\right], \tag{2.5}$$

where $\mathcal{H}(\{\sigma\},\{Q\})$ is

$$\mathcal{H}(\{\sigma\},\{Q\})=\sum_l (E_{\rm FC}-\sqrt{S}\,Q_l)(\sigma_l+\tfrac{1}{2}) +\tfrac{1}{2}\sum_l Q_l^2-\tfrac{1}{2}\sum_{l,l'} K_{ll'}Q_lQ_{l'}\ . \tag{2.6}$$

In Eqs. (2.5) and (2.6), we introduce the spin σ_l which corresponds to the two alternative g and e states as follows:

$$\sigma_l=\begin{cases}+\frac{1}{2} & e \text{ state}\\ -\frac{1}{2} & g \text{ state.}\end{cases} \tag{2.7}$$

The trace ${\rm Tr}_{\{\sigma\}}$ is over the spin configurations and $\mathcal{D}Q$ is $\prod_l dQ_l$. We shift the origin of the displacement by

$$Q_l=Q_l'+\frac{\sqrt{S}}{2(1-K)}\ , \tag{2.8}$$

where $K=\sum_{l'} K_{ll'}$. The Hamiltonian in Eq. (2.6) is rewritten using Q_l' as follows:

$$\mathcal{H}(\{\sigma\},\{Q'\})=\sum_l \left[E_{\rm FC}-\frac{S}{2(1-K)}-\sqrt{S}Q_l'\right]\sigma_l + \tfrac{1}{2}\sum_l Q_l'^2-\tfrac{1}{2}\sum_{l\neq l'} K_{ll'}Q_l'Q_{l'}' \ . \quad (2.9)$$

From this equation, the symmetry of the model with respect to the following transformation is evident:

$$\sigma_l \leftrightarrow -\sigma_l \ , \quad (2.10a)$$

$$Q_l' \leftrightarrow -Q_l' \ , \quad (2.10b)$$

$$S \leftrightarrow S \ , \quad (2.10c)$$

$$K_{ll'} \leftrightarrow K_{ll'} \ , \quad (2.10d)$$

$$E_{\rm FC} \leftrightarrow -E_{\rm FC}+\frac{S}{1-K} \ . \quad (2.10e)$$

Equation (2.10a) corresponds to the exchange of g and e states, and on the line $2E_{\rm FC}=2/(1-K)$, the model is symmetric with respect to this exchange. Therefore the region $\tilde{S}\equiv S/E_{\rm FC}\leq 2(1-K)$ is enough if we choose the g state properly, though we have discussed a wider range $\tilde{S}\leq 2$ simply to make the phase diagram rectangular.

The Gaussian integrations with respect to Q's are easily performed to give the following result:

$$Z \propto {\rm Tr}_{\{\sigma\}} \exp\left[-\frac{\mathcal{H}_{\rm eff}(\{\sigma\})}{k_B T}\right] , \quad (2.11)$$

where the effective Hamiltonian is given by

$$\mathcal{H}_{\rm eff}(\{\sigma\})=-h\sum_l \sigma_l-\tfrac{1}{2}\sum_{l\neq l'} J_{ll'}\sigma_l\sigma_{l'} \ . \quad (2.12)$$

This is nothing but the Ising model, and the "field" h and the exchange $J_{ll'}$ are given as follows:

$$h=-E_{\rm FC}+\frac{S}{2(1-K)} \ , \quad (2.13a)$$

$$J_{ll'}=\frac{S}{N}\sum_{\mathbf{k}}\frac{\cos[\mathbf{k}\cdot(\mathbf{R}_l-\mathbf{R}_{l'})]}{\omega_{\mathbf{k}}^2} \ , \quad (2.13b)$$

where $\mathbf{R}_l$ is the lattice vector of the lth site, and $\omega_{\mathbf{k}}^2$ is given by

$$\omega_{\mathbf{k}}^2=1-K(\mathbf{k})=1-\sum_{l'} K_{ll'}\exp[i\mathbf{k}\cdot(\mathbf{R}_l-\mathbf{R}_{l'})] \ . \quad (2.14)$$

The summation with respect to the wave vector $\mathbf{k}$ runs over the first Brillouin zone, i.e., $-\pi\leq k_x,k_y,k_z\leq\pi$. From Eq. (2.14), we find

$$\omega_{\mathbf{k}=0}=1-K \ , \quad (2.15)$$

and K should be less than unity for the stability of the system.

Already much is known about this Ising model. We summarize below the mean-field approximation on this model. The mean-field approximation is equivalent to replacing $J_{ll'}$ by the infinite ranged constant value as follows:

$$J_{ll'}\rightarrow\frac{1}{N}\sum_{l'(\neq l)} J_{ll'}=\frac{1}{N}\frac{SK}{1-K}\equiv\frac{J}{N} \ . \quad (2.16)$$

It should be noted that Eq. (2.16) can be obtained also by replacing $K_{ll'}$ by K/N in the original Hamiltonian (2.1).

(i) The transition temperature T_c in the absence of the field h is given by

$$k_B T_c=\frac{J}{4}=\frac{SK}{4(1-K)} \ . \quad (2.17)$$

(ii) Below this temperature, the free energy $F(M)$ as a function of the magnetization $M=\langle\sigma_l\rangle\equiv n_e-\frac{1}{2}$ has double minima. Applying the "magnetic field" h, the relative height of the two minima of the free energy $F(M)-hM$ changes, and at last one of the minima vanishes. We can expect the switching phenomena only in the case of double minima in $F(M)-hM$. The boundary of the switching and nonswitching regions is given by Eq. (A8) in Appendix A. It should be noted that the condition for the switching Eq. (A8) is reduced to

$$|h|<\frac{J}{2} \ , \quad (2.18)$$

at zero temperature, which is nothing but the stability condition of the uniform metastable state against the single spin flip.

To discuss further the nonequilibrium dynamics of the system, we introduce the stochastic dynamics to the Ising model (kinetic Ising model). We will specify the transition rates between the g (down spin) and e (up spin) states of the kinetic Ising model in the next subsection.

B. Kinetic Ising model

In this section we discuss the transition probabilities between g and e states. They are composed of two contributions, i.e., the optical and thermal processes.

The transition probability $P_{e\rightarrow g}^{\rm opt}$ ($P_{g\rightarrow e}^{\rm opt}$) from e state (g state) to g state (e state) of the lth molecule via the *optical* transitions are given by the thermal distribution function of excited and ground states P_e and P_g, the probabilities for the upward (downward) transitions $P^{\rm up}$'s ($P^{\rm down}$'s) as follows (the derivation is given in Appendix B):

$$P_{e\rightarrow g}^{\rm opt}=\int dQ_l P_e(Q_l)[P_{e\rightarrow g}^{\rm down}(Q_l)\Theta(E_{\rm FC}-\sqrt{S}Q_l) + P_{e\rightarrow g}^{\rm up}(Q_l)\Theta(\sqrt{S}Q_l-E_{\rm FC})] \ , \quad (2.19a)$$

$$P_{g\rightarrow e}^{\rm opt}=\int dQ_l P_g(Q_l)[P_{g\rightarrow e}^{\rm up}(Q_l)\Theta(E_{\rm FC}-\sqrt{S}Q_l) + P_{g\rightarrow e}^{\rm down}(Q_l)\Theta(\sqrt{S}Q_l-E_{\rm FC})] \ . \quad (2.19b)$$

Only the vertical transition with respect to Q_l is possible (Franck-Condon principle),[15] and the total transition probabilities are given by the integral with respect to Q_l. The unit step $\Theta(x)$ appearing in the above expressions specifies which of e and g is lower in energy for each Q_l. It should be noticed that the above transition probabilities satisfy the condition of detailed balance at each site l

as is given below, because $P^{\rm down}(Q_l)$'s and $P^{\rm up}(Q_l)$'s satisfy the condition of detailed balance for each Q_l and we assume the thermal equilibrium of Q_l within g and e states:

$$\frac{P^{\rm opt}_{e\to g}}{P^{\rm opt}_{g\to e}}=\exp\left[\frac{E_e-E_g}{k_BT}\right]. \tag{2.20}$$

The emission spectrum $\hat{I}_{e\to g}(E)$ $[\hat{I}_{g\to e}(E)]$ when the initial state is e state (g state) is given by

$$\hat{I}_{e\to g}(E)\propto P_e\left[\frac{E_{\rm FC}-E}{\sqrt{S}}\right]P^{\rm down}_{e\to g}\left[\frac{E_{\rm FC}-E}{\sqrt{S}}\right] -P_e\left[\frac{E_{\rm FC}+E}{\sqrt{S}}\right]P^{\rm up}_{e\to g}\left[\frac{E_{\rm FC}+E}{\sqrt{S}}\right], \tag{2.21a}$$

$$\hat{I}_{g\to e}(E)\propto P_g\left[\frac{E_{\rm FC}+E}{\sqrt{S}}\right]P^{\rm down}_{g\to e}\left[\frac{E_{\rm FC}+E}{\sqrt{S}}\right] -P_g\left[\frac{E_{\rm FC}-E}{\sqrt{S}}\right]P^{\rm up}_{g\to e}\left[\frac{E_{\rm FC}-E}{\sqrt{S}}\right]. \tag{2.21b}$$

On the other hand, the *thermal* transition rates are free from the Franck-Condon principle. We derive the forms of the thermal transition probabilities of the lth molecule as follows. The thermal transition probabilities are assumed to be the attempt frequency τ_t^{-1} times the activation factor:

$$P^{\rm th}_{e\to g}=\frac{1}{\tau_t}\exp\left[-\frac{E_c-E_e}{k_BT}\right], \tag{2.22a}$$

$$P^{\rm th}_{g\to e}=\frac{1}{\tau_t}\exp\left[-\frac{E_c-E_g}{k_BT}\right], \tag{2.22b}$$

where E_c, E_e, and E_g are the energy of the cross point of the two parabolas, the energy of the bottom of the e parabola and g parabola, respectively, for lth site in Fig. 1. The attempt frequency τ_t^{-1} is of the order of the Debye frequency ($\sim 10^{13}$ Hz) and is much larger than τ_r^{-1} in Eqs. (B1) ($\sim 10^9$ Hz). The thermal transition probabilities $P^{\rm th}$'s, however, can be much smaller than the optical transition probabilities $P^{\rm opt}$'s due to the activation factor. The energy differences E_c-E_e and E_c-E_g are the potential barriers seen from the bottom of the e parabola and g parabola, respectively. It should be noticed that also $P^{\rm th}_{e\to g}$ and $P^{\rm th}_{g\to e}$ satisfy the condition of detailed balance at each site l:

$$\frac{P^{\rm th}_{e\to g}}{P^{\rm th}_{g\to e}}=\exp\left[\frac{E_e-E_g}{k_BT}\right]. \tag{2.23}$$

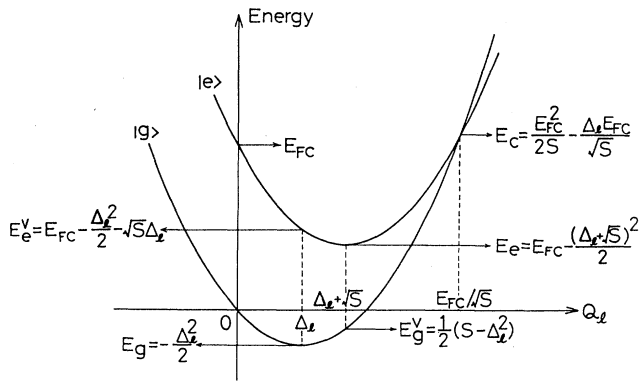

FIG. 1. The energy diagram of the localized electronic two levels $|e\rangle$ and $|g\rangle$ against the displacement Q_l.

C. Nucleation process in the kinetic Ising model

Now we consider the effects of the fluctuations which enter when the interaction $K_{ll'}$ is short ranged. We assume two kinds of coupling constants $J_\parallel$ and $J_\perp$ for the exchange integral $J_{ll'}$ in (2.13b) parallel and perpendicular to the chain, respectively. Applying the nucleation theory[16] to this anisotropic three-dimensional system, the critical droplet size is

$$L_\parallel\sim\frac{J_\parallel^{2/3}J_\perp^{1/3}}{|h|}, \tag{2.24a}$$

along the chain and

$$L_\perp\sim\frac{J_\parallel^{1/6}J_\perp^{5/6}}{|h|}, \tag{2.24b}$$

perpendicular to the chain, respectively. The quasi-one-dimensionality reflects in the inequality $J_\perp\ll J_\parallel$ which results in $L_\perp/L_\parallel=(J_\perp/J_\parallel)^{1/2}\ll 1$. The above arguments, however, are based on the continuum approximation which fails when $L_\perp<1$, i.e., $J_\parallel^{1/6}J_\perp^{5/6}<|h|$. In this case, the nucleation process occurs in each chain separately because the confining potential from the neighboring chains, which is of the order $J_\perp$, is small compared to the energy difference $|h|$ due to the inequality $1\ll(J_\parallel/J_\perp)^{1/6}<|h|/J_\perp$. The one-dimensional nucleation process is quite different from that for higher dimensions. The cost in the surface energy does not depend on the linear size L of the droplet, and the continuum approximation cannot be applied. We have already discussed this case in detail and the readers are referred to Refs. 12 and 13.

We restrict our discussion to the case $L_\perp>1$ below. The size $N_{\rm cr}$ and the energy $E_{\rm cr}$ of the critical droplet are given by

$$N_{\rm cr}\sim L_\parallel L_\perp^2\sim\frac{J_\parallel J_\perp^2}{|h|^3}, \tag{2.25a}$$

$$E_{\rm cr}\sim N_{\rm cr}|h|\sim\frac{J_\parallel J_\perp^2}{h^2}. \tag{2.25b}$$

The rate τ_m^{-1} of the appearance of the critical droplet due to the thermal fluctuations is given by

$$\tau_m^{-1}\sim\tau_t^{-1}\exp\left[-\frac{E_{\rm cr}}{k_BT}\right]. \tag{2.26}$$

When we increase the ratio of the excited molecules n_e from zero to finite value, the probability $P_{\rm cr}$ of finding the

critical droplet is given by

$$P_{\rm cr}\sim n_e^{N_{\rm cr}}=\exp\left[-\frac{J_\parallel J_\perp^2}{|h|^3}\ln\left[\frac{1}{n_e}\right]\right] . \tag{2.27}$$

When $P_{\rm cr}$ has appreciable values or we are interested in the time scale longer than or of the order of τ_m, we cannot neglect the spontaneous growth of the droplet beyond the critical size even practically. It is necessary that $N_{\rm cr}$ is large compared to unity for the probability $P_{\rm cr}$ to be much smaller than unity and the time τ_m is quite long. This means that $J_\parallel J_\perp^2$ is much larger than $|h|$.

Exactly speaking, the system always relaxes to the absolutely stable state and there is no switching if we wait for infinitely long time. Therefore the switching phenomenon is a nonequilibrium process depending on the time scale one is interested in. There are several characteristic time scales inherent in our model which will be discussed in the next section. If the lifetime of the metastable state due to the nucleation process τ_m given in Eq. (2.26) is much longer than these time scales, we neglect the fluctuation to describe the dynamics of the photoinduced structure changes. That is, we apply the dynamical mean-field approximation to the kinetic Ising model as will be discussed in Sec. III.

III. DYNAMICS OF THE PHOTOINDUCED STRUCTURE CHANGES

We now apply the mean-field approximation to the kinetic Ising model. The influence from the surrounding sites on the transition probabilities at lth site is replaced by the average value. Therefore Δ_l in Fig. 1 is replaced by its average value $\Delta=K\langle Q\rangle$ with $K=\sum_{l'}K_{ll'}$ and $\langle Q\rangle$ is the average value of the displacement Q_l's over all the sites. Then, we will concentrate on the total number of e sites N_e. The number of g sites N_g is of course given by $N-N_e$, where N is the total number of sites. The average value of Q with respect to the thermal distribution is the location of the bottom of each parabola. Therefore the mean displacement $\langle Q\rangle$ is expressed by N_e as

$$\begin{aligned}\langle Q\rangle&=\frac{1}{N}[N_e(\Delta+\sqrt{S}\,)+N_g\Delta]\\&=\Delta+\sqrt{S}\,\frac{N_e}{N}\\&=K\langle Q\rangle+\sqrt{S}\,n_e ,\end{aligned} \tag{3.1}$$

where $n_e=N_e/N$ is the ratio of the e sites.

Solving Eq. (3.1) for $\langle Q\rangle$, we obtain

$$\Delta=K\langle Q\rangle=\frac{K\sqrt{S}}{1-K}n_e . \tag{3.2}$$

Therefore the state is specified only by n_e in our mean-field picture.

We investigate the dynamics of the system under and after the optical pumping. Our equation which describes the time evolution of the system is the rate equation for $n_e(t)$:

$$\begin{aligned}\frac{d}{dt}n_e(t)=&I(t)+(P^{\rm th}_{g\to e}+P^{\rm opt}_{g\to e})[1-n_e(t)]\\&-(P^{\rm th}_{e\to g}+P^{\rm opt}_{e\to g})n_e(t) ,\end{aligned} \tag{3.3}$$

where $I(t)$ is the optical pumping, and is positive when the e state is created while it is negative when the g state is created. The notations $P^{\rm th}_{e\to g}$ ($P^{\rm th}_{g\to e}$) and $P^{\rm opt}_{e\to g}$ ($P^{\rm opt}_{g\to e}$) are the transition probabilities from e state (g state) to g state (e state) via the thermal processes and the optical processes, respectively, given in the preceding section with the site dependent Δ_l being replaced by the uniform value Δ.

In this section we consider the case of low-temperature $\tilde{T}\equiv k_BT/S\ll 1$. This case is experimentally relevant because the systems in which the structure changes occur have the large lattice relaxation energy compared with the room temperature. We neglect the finite temperature effect on the optical transitions. At $T=0$, only the spontaneous emission survives and Eqs. (2.19) become

$$P^{\rm opt}_{e\to g}=\frac{1}{\tau_r}F(\Delta+\sqrt{S}\,)\Theta(E_{\rm FC}-S-\sqrt{S}\,\Delta) , \tag{3.4a}$$

$$P^{\rm opt}_{g\to e}=\frac{1}{\tau_r}F(\Delta)\Theta(\sqrt{S}\,\Delta-E_{\rm FC}) , \tag{3.4b}$$

where τ_r is the radiative lifetime and the function F is given in Appendix B. Equations (2.21) become

$$\begin{aligned}\hat{I}_{e\to g}(E)\propto&\frac{1}{\tau_r}F(\Delta+\sqrt{S}\,)\Theta(E_{\rm FC}-S-\sqrt{S}\,\Delta)\\&\times\delta(E-E_{\rm FC}+S+\sqrt{S}\,\Delta) ,\end{aligned} \tag{3.5a}$$

$$\hat{I}_{g\to e}(E)\propto\frac{1}{\tau_r}F(\Delta)\Theta(\sqrt{S}\,\Delta-E_{\rm FC})\delta(E+E_{\rm FC}-\sqrt{S}\,\Delta) , \tag{3.5b}$$

where the energies which appear in the Θ and δ functions are nothing but vertical energy differences in Fig. 1 as

$$E_e-E_g^V=E_{\rm FC}-S-\sqrt{S}\,\Delta , \tag{3.6a}$$

$$E_g-E_e^V=\sqrt{S}\,\Delta-E_{\rm FC} , \tag{3.6b}$$

where E_g^V and E_e^V are defined in Fig. 1.

Whether the spontaneous emission is possible or not depends on the relative relation of the two parabolas in Fig. 1. Figure 2 shows the four cases of the relative relations of two parabolas. The spontaneous emission is possible only in cases (a) and (d), and is represented by the

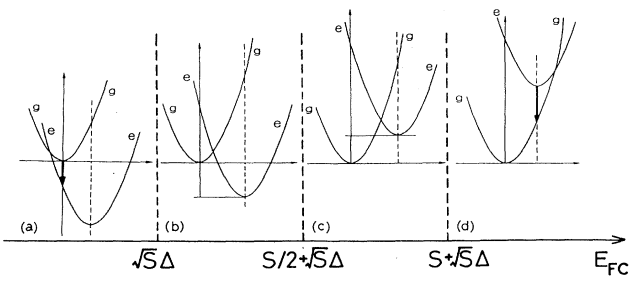

FIG. 2. Four types of the relative location between two parabolas in the energy diagrams. Downward arrows in (a) and (d) denote the spontaneous emissions. Cases (b) and (c) are optically stable in the zero-temperature limit $\tilde{T}\ll 1$.

downward arrows. In cases (b) and (c), the system is optically stable against the spontaneous emission, and its condition is written as

$$\sqrt{S}\,\Delta=\sqrt{S}K\langle Q\rangle<E_{\rm FC}<S+\sqrt{S}\,\Delta=S+\sqrt{S}K\langle Q\rangle\ . \tag{3.7}$$

Using Eqs. (3.1), Eq. (3.7) is transformed into

$$n_L\equiv\frac{1-K}{K}\frac{1-\tilde{S}}{\tilde{S}}<n_e<\frac{1-K}{K}\frac{1}{\tilde{S}}\equiv n_U\ . \tag{3.8}$$

At finite temperature, $P_g(Q)$ and $P_e(Q)$ have the width of order $(k_BT)^{1/2}$, and the thermal occupation of the photon cannot be neglected for $|\sqrt{S}Q-E_{\rm FC}|<k_BT$. Therefore the effects of the width of the distributions $P_g(Q)$ and $P_e(Q)$ dominate even for $k_BT\ll S$, but its effect is restricted to the small region near the crossing point where the thermal transitions prevail. A detailed discussion of the effects at finite temperature will be given in Sec. IV.

As for the thermal transition probabilities, the activation energies in Eqs. (2.22) are given by

$$E_c-E_g=\frac{S}{2}\left[\frac{K}{1-K}n_e-\frac{1}{\tilde{S}}\right]^2$$

$$=\frac{S}{2}\left[\frac{K}{1-K}\right]^2(n_e-n_U)^2\ , \tag{3.9a}$$

$$E_c-E_e=\frac{S}{2}\left[\frac{K}{1-K}n_e-\frac{1-\tilde{S}}{\tilde{S}}\right]^2$$

$$=\frac{S}{2}\left[\frac{K}{1-K}\right]^2(n_e-n_L)^2\ . \tag{3.9b}$$

The ratio of e state n_e lies between 0 and 1, and the relative relations of n_L,n_U and 0,1 results in the qualitative difference in the dynamics of the structure change. Figure 3 summarizes the results. As was discussed in Sec. II, the region $h<0$, i.e., $\tilde{S}<2(1-K)$, is enough to cover all the cases because of the symmetry of our model for exchanging g and e states. However, we extend the plane to $\tilde{S}<2$ simply to make the phase diagram rectangular. The relations $0<n_U$ and $n_L<n_U$ always holds, and there are three boundaries which correspond to $n_U=1$, $n_L=0$, and $n_L=1$, respectively. Together with the condition Eq. (2.18) for switching at zero temperature, the plane is divided into seven regions as is shown in Fig. 3. Here we stress again that the mean-field approximation works only when $|h|\ll J$, i.e., near the diagonal line $\tilde{S}=2(1-K)$, and fails in the nonswitching regions E, F, and G.

As has been discussed above, the collective nature of the system is built-in through the dependence of the transition probabilities upon n_e and Eq. (3.3) is written as follows:

$$\frac{d}{dt}n_e(t)=I(t)+u(n_e)\ . \tag{3.10}$$

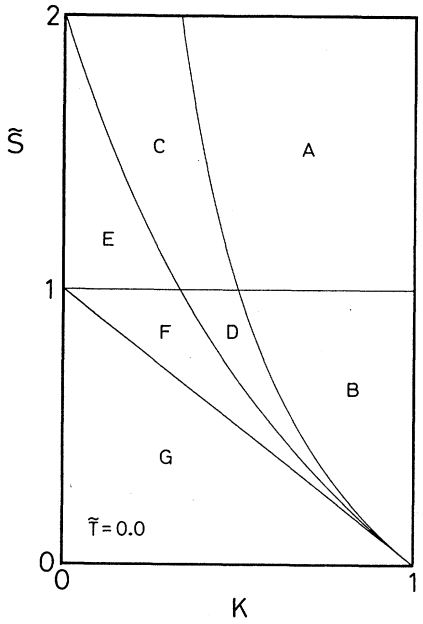

FIG. 3. Characteristics of the structure changes at zero temperature on the parameter space $(K,\tilde{S})$. Regions $A-D$ are switching and $E-G$ nonswitching regions.

The function $u(n_e)$ is explicitly given by

$$u(n_e)=\left[\frac{1}{\tau_t}\exp\left[-\frac{\alpha}{2}(n_e-n_U)^2\right]+\frac{1}{\tau_r}F(\Delta)\Theta(n_e-n_U)\right](1-n_e)$$

$$-\left[\frac{1}{\tau_t}\exp\left[-\frac{\alpha}{2}(n_L-n_e)^2\right]+\frac{1}{\tau_r}F(\sqrt{S}+\Delta)\Theta(n_L-n_e)\right]n_e\ . \tag{3.11}$$

We have used the zero-temperature forms for the optical transition probabilities, and assume that $F(\Delta+\sqrt{S})$ and $F(\Delta)$ are unity except near the crossing point where they vanish smoothly. The coefficient α is defined as

$$\alpha\equiv\frac{1}{\tilde{T}}\left[\frac{K}{1-K}\right]^2\ , \tag{3.12}$$

where $\tilde{T}\equiv k_BT/S$. At low temperature $\tilde{T}\ll 1$, α is much larger than unity except the small region $K\ll 1$ where the physical properties are almost the same as noninteracting localized electron-lattice systems. By using $U(n_e)$, which is the minus of the indefinite integral of $u(n_e)$, Eq. (3.10) is rewritten as

$$\frac{d}{dt}n_e(t)=I(t)-\frac{dU(n_e)}{dn_e}\ . \tag{3.13}$$

As is evident from Eq. (3.13), the function $U(n_e)$ plays the role of the potential, and the system relaxes to a

minimum of $U(n_e)$ without the optical pumping. It is an easy task to see that $U(n_e)$ has two minima separated by the barrier in the switching region while it has only one minimum outside the switching region in Fig. 3. In this section we neglect the small shift of the boundaries due to the finite temperature, i.e., we exclude the region near the boundaries from consideration. Therefore we base our discussion on the phase diagram (Fig. 3) at zero temperature. The functions $u(n_e)$ and hence $U(n_e)$ are different qualitatively in each region of Fig. 3. We take the region D as an example, and discuss the dynamics in detail. The extension to other regions is straightforward.

When we neglect the correction of the order of $\exp(-c\alpha)$ with c being a constant of order unity, the two minima of $U(n_e)$ are at $n_e=0$ and $n_e=1$. The function $u(n_e)$ is shown schematically in Fig. 4 in region D of Fig. 3. The negative contribution $u_-(n_e)$ is the sum of the Gaussian centered at $n_e=n_L$ with the width $1/\sqrt{\alpha}$ and the contribution from $P^{\rm opt}_{e\to g}$ which is the straight line starting from the origin ($n_e=u=0$) which vanishes smoothly at $n_e=n_L$. Therefore $u(n_e)$ has the minimum value $u_{\rm min}=-\tau_t^{-1}n_L$ at $n_e=n_{\rm min}=n_L$.

The positive contribution $u_+(n_e)$ on the other hand, is only the tail of the Gaussian centered at $n_e=n_U$ with the width $1/\sqrt{\alpha}$ and the contribution from $P^{\rm opt}_{g\to e}$ is absent because $n_U>1$. Therefore $u(n_e)$ has the maximum value $u_{\rm max}$ at $n_e=n_{\rm max}$ as follows:

$$u_{\rm max}=u_+\left[n_{\rm max}=1-\frac{1}{\alpha(n_U-1)}\right]$$
$$=\frac{1}{\tau_t\alpha(n_U-1)}\exp\left[-\frac{\alpha}{2}(n_U-1)^2-1\right]. \quad (3.14)$$

Here note that $u_{\rm max}$ is much smaller than $|u_{\rm min}|$, and $1-n_{\rm max}$ is much smaller than $n_{\rm min}$. This difference results in the difference between the dynamics of photoinduced structure changes from $n_e=0$ and from $n_e=1$. Between n_L and n_U, $u(n_e)$ is composed of the tails of the two Gaussians, and is of the order of $\exp(-c\alpha)$ with c being a constant of order unity. The location $n_{\rm cr}$ of the maximum of the potential $U(n_e)$ is the solution of $u(n_e)=0$ which lies between n_L and n_U, i.e.,

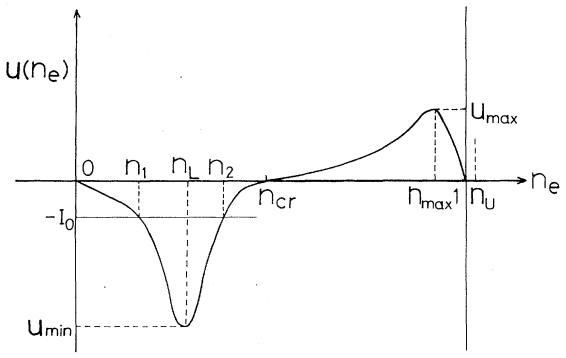

FIG. 4. Schematic figures of the function $u(n_e)$ in the D region of Fig. 3.

$$\exp\left[-\frac{\alpha}{2}(n_{\rm cr}-n_U)^2+\ln(1-n_{\rm cr})\right]$$
$$=\exp\left[-\frac{\alpha}{2}(n_{\rm cr}-n_L)^2+\ln(n_{\rm cr})\right]. \quad (3.15)$$

From Eq. (3.15) we obtain

$$n_{\rm cr}=\tfrac{1}{2}(n_L+n_U)+O\left[\frac{1}{\alpha}\right]$$
$$=\frac{1-K}{K}\frac{1-\tilde{S}/2}{\tilde{S}}+O\left[\frac{1}{\alpha}\right]. \quad (3.16)$$

Note that $n_{\rm cr}$ lies between 0 and 1 in the switching region, and is a decreasing function of K and $\tilde{S}$ vanishing on the two lines $\tilde{S}=2$ and $K=1$.

Now, we consider the dynamics of the system under and after the optical pumping $I(t)$. Starting from the minimum point $n_e=0$ or 1, we apply the following optical pumping:

$$I(t)=\begin{cases}I_0 & \text{for } 0\le t<t_0\\ 0 & \text{for } t_0\le t.\end{cases} \quad (3.17)$$

The intensity I_0 is the rate of the creation of e state ($I_0>0$) or g state ($I_0<0$). The product of $|I_0|$ and t_0 is the total number of the e-state (g-state) sites created by the pumping divided by the total number of sites. In Eqs. (3.3), (3.10), and (3.13), we neglect the saturation of the absorption, and a more exact expression of Eq. (3.10) is

$$\frac{d}{dt}n_e(t)=\begin{cases}I(t)(1-n_e)\Theta(n_U-n_e)+u(n_e) & \text{for } I(t)>0\\ I(t)n_e\Theta(n_e-n_L)+u(n_e) & \text{for } I(t)<0.\end{cases} \quad (3.18)$$

Here, we assume the constant pumping Eq. (3.17) with the restriction that n_e does not exceed n_U from below (n_e does not exceed n_L from above).

Then the differential equation (3.10) can be integrated as follows:

$$\int_{n_i}^{n_e(t)}\frac{dx}{I_0+u(x)}=t, \quad 0<t<t_0 \quad (3.19a)$$

$$\int_{n_e(t_0)}^{n_e(t)}\frac{dx}{u(x)}=t-t_0, \quad t_0<t \quad (3.19b)$$

where n_i is the initial value of n_e, and is 0 or 1.

At first we consider the optical pumping from the initial value $n_i=0$. From 0 to $n_{\rm cr}$, the function $u(n_e)$ is negative and there are two cases according to the sign of the integrand in Eq. (3.19a).

When I_0 is less than $|u_{\rm min}|$, $I_0+u(n_e)$ becomes zero at two values n_1 and n_2 (Fig. 4), and the following integral diverges:

$$\lim_{n_e\to n_1-0}\int_{n_i}^{n_e}\frac{dx}{I_0+u(x)}=\infty. \quad (3.20)$$

Equation (3.20) means that however long we apply the optical pumping, n_e does not exceed the value n_1, i.e.,

$n_e(t_0)<n_1$. After the pumping is switched off, the system always relaxes to the initial value $n_i=0$. Therefore we cannot switch the system from the initial value $n_i=0$ to the final value $n_f=1$ however long we continue the optical pumping as long as the pumping intensity I_0 is less than the threshold value $I_{\rm th}=|u_{\rm min}|=n_L/\tau_t$. After the switchoff of the pumping, n_e relaxes to its initial value $n_i=0$ within the radiative lifetime τ_r because the spontaneous emission dominates at low temperatures.

When I_0 is greater than $|u_{\rm min}|$, on the other hand, $I_0+u(n_e)$ is always positive between $n_e=0$ and $n_{\rm cr}$, and $n_e(t)$ is monotonically increasing without the saturation for $0<t<t_0$ as is evident from Eq. (3.19a). After we switch off the optical pumping at $t=t_0$, n_e relaxes to the final value $n_f=0$ when $n_e(t_0)<n_{\rm cr}$ and to $n_f=1$ when $n_e(t_0)>n_{\rm cr}$. Therefore there is a critical value of the duration time t_0 above which the system is switched from $n_i=0$ to $n_f=1$, which is determined by the following integral:

$$t_{\rm cr}=t_{\rm cr}(I_0)=\int_{n_i}^{n_{\rm cr}}\frac{dx}{I_0+u(x)} . \tag{3.21}$$

As a function of I_0, the threshold time $t_{\rm cr}$ is inversely proportional to I_0 for large I_0 and diverges as $I_0\to|u_{\rm min}|+0$ as is shown in Fig. 5. The asymptotic form of $t_{\rm cr}$ near the diverging point $I_{\rm th}$ is given as follows:

$$t_{\rm cr}\sim(I_0-I_{\rm th})^{-1/2} , \tag{3.22a}$$

with

$$I_{\rm th}=|u_{\rm min}|\frac{n_L}{\tau_t}=\frac{1}{\tau_t}\frac{1-K}{K}\frac{1-\tilde{S}}{\tilde{S}} . \tag{3.22b}$$

Now we discuss the relaxation after the switchoff of the pumping. If the duration time t_0 is shorter than $t_{\rm cr}(I_0)$, n_e relaxes to 0 accompanied by the spontaneous emission within the radiative lifetime τ_r. If t_0 is longer than $t_{\rm cr}(I_0)$, on the other hand, n_e relaxes to 1 after the switchoff. The relaxation proceeds only through the thermal transitions, and it is slow in the early stage and will be accelerated gradually because the activation energy decreases and $P^{\rm th}_{g\to e}$ increases as n_e increases. Therefore the relaxation time τ is determined mainly by the early stage and is given by

$$\tau\simeq\int_{n_e(t_0)}^{1}\tau_t\exp\left[\frac{\alpha}{2}(x-n_U)^2\right]dx$$
$$\simeq\frac{\tau_t}{\alpha[n_U-n_e(t_0)]}\exp\left[\frac{\alpha}{2}[n_e(t_0)-n_U]^2\right] . \tag{3.23}$$

Here note that the relaxation time τ is strongly dependent on the number of the excited molecules $n_e(t_0)$ just after the switchoff at $t=t_0$ as well as the temperature and material parameters.

The dynamics of the system with the optical pumping from the initial value $n_i=1$ can be similarly analyzed. The differences come from the fact that the spontaneous emission is forbidden near $n_e=1$. As the result, $I_{\rm th}=u_{\rm max}$ given in Eq. (3.14) is small compared with Eq. (3.22b), and is strongly temperature dependent. The relaxation after the switchoff of the optical pumping occurs only through the thermal transitions for both directions, and the relaxation time τ is given by

$$\tau\simeq\frac{\tau_t}{\alpha[n_U-n_e(t_0)]}\exp\left[\frac{\alpha}{2}[n_e(t_0)-n_U]^2\right] , \tag{3.24a}$$

to $n_e=1$ when $t_0<t_{\rm cr}(I_0)$ and

$$\tau\simeq\frac{\tau_t}{\alpha[n_e(t_0)-n_L]}\exp\left[\frac{\alpha}{2}[n_e(t_0)-n_L]^2\right] , \tag{3.24b}$$

to $n_e=0$ when $t_0>t_{\rm cr}(I_0)$ or $I_0<I_{\rm th}$.

We have discussed the dynamics of the photoinduced structure changes in region D of Fig. 3. The extension to other regions is straightforward. The location of n_L and n_U defined in Eq. (3.8) almost determines the dynamics. We show in Fig. 6 the shape of the potential $U(n_e)$ for the respective region as well as the location of n_L and n_U.

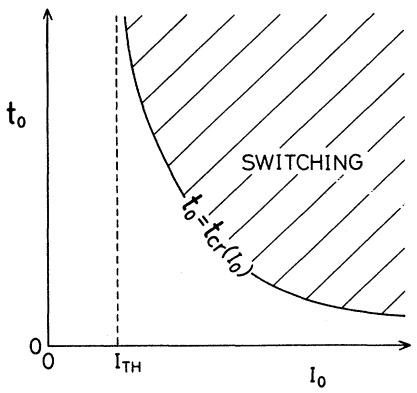

FIG. 5. The threshold behavior of the switching in the intensity (I_0)—duration time (t_0) plane. In the hatched region, the system can switch to the other state.

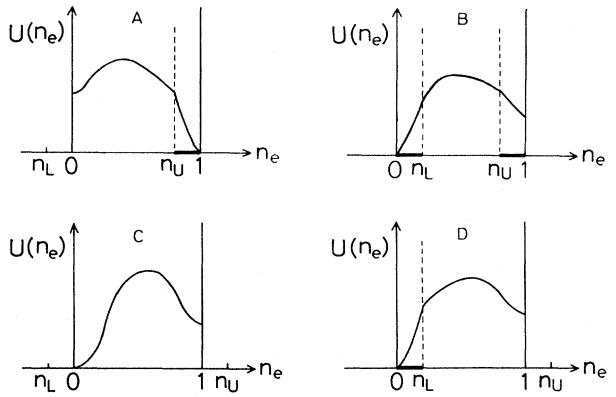

FIG. 6. Schematic figures of the potential function $U(n_e)$ in the switching regions $A-D$ at zero temperature. Thick lines along the abscissa mean the spontaneous emission occurs in the relaxation processes.

Thick lines along the abscissa mean that the spontaneous emission occurs in the relaxation process. It would be an easy task to imagine the dynamics of the system with the optical pumping for regions A, B, and C as we analyzed for region D. In the discussion above, there are three characteristic time scales: (1) The radiative lifetime τ_r, (2) the inverse of the pumping rate I_0^{-1} or the duration time t_0, and (3) the characteristic lifetime due to the thermal transitions $\tau_1=\tau_t\exp(\alpha)$. One should compare these three time scales with τ_m given in Eq. (2.26) to judge the applicability of our mean-field theory.

In the nonswitching regions E, F, and G, the excited molecules are rapidly deexcited to the ground state through the thermal transitions in region E and through the spontaneous emission as well as the thermal transitions in regions F and G. Although the mean-field approximation fails in these regions, the above distinction between region E and regions F and G remains true when we consider the relaxation of a single excited molecule.

IV. DISCUSSION

A. Phase diagram and dynamics at general temperature

In this section we discuss the finite temperature effects on the phase diagrams and on the dynamics of the photoinduced structure changes. First, we list below what occurs generally when the temperature $\tilde{T}$ is raised.

(i) The switching region shrinks and is located at the large K and small $\tilde{S}$ ($K\simeq 1$, $\tilde{S}\simeq 0$) part of the parameter plane.

(ii) The location of the minima of the potential $U(n_e)$ departs from the end points $n_e=0$ and/or $n_e=1$ toward the middle.

(iii) The relative importance of the thermal transitions increases drastically, and hence the relaxation time becomes shorter.

(iv) Due to the thermal distribution of Q around the bottom of the potential of the parabola with the width $(k_BT)^{1/2}$, the spontaneous emission is always possible. Therefore the criteria by n_L and n_U become ambiguous with the width of an order of δn_e which is obtained by equating the shift of the parabola $\delta\Delta$ with $(k_BT)^{1/2}$:

$$\delta\Delta=\frac{\sqrt{\tilde{S}}K}{1-K}\delta n_e\simeq(k_BT)^{1/2}\ . \tag{4.1}$$

From Eq. (4.1), δn_e is given by

$$\delta n_e\simeq\frac{1-K}{K}\sqrt{\tilde{T}}\ . \tag{4.2}$$

Taking into account the above situations, we discuss the phase diagram at finite temperatures.[17,18] We show in Figs. 7(a) and 7(b) the two typical phase diagrams with (a) $\tilde{T}=0.05$ and (b) $\tilde{T}=0.3$. It is easily seen that the change between Figs. 7(a) and 7(b) occurs at $\tilde{T}=\frac{1}{4}$. The shaded regions represent the crossover region between the radiative and nonradiative regions, and are given as follows using the criterion Eq. (4.2) with the factor $\frac{1}{2}$ chosen rather arbitrarily:

$$|n_U-1|\le\tfrac{1}{2}\delta n_e\ , \tag{4.3a}$$

$$|n_L-1|\le\tfrac{1}{2}\delta n_e\ , \tag{4.3b}$$

$$|n_L|\le\tfrac{1}{2}\delta n_e\ . \tag{4.3c}$$

In Fig. 7, the switching region C and then region D disappear as the temperature increases. The switching

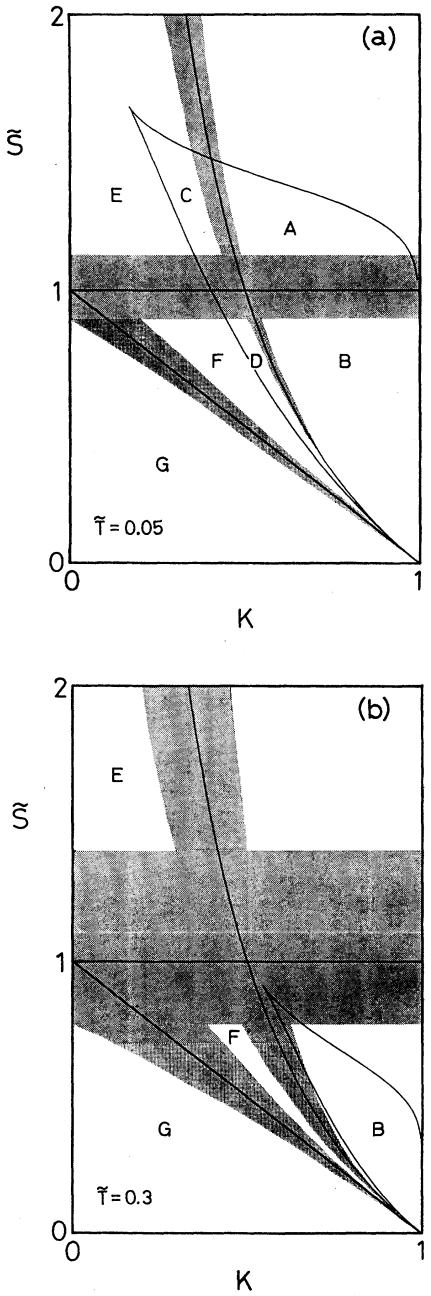

FIG. 7. Characteristics of the structure changes at (a) $\tilde{T}=0.05$ and (b) $\tilde{T}=0.3$ on the parameter space $(K,\tilde{S})$. The dark regions represent crossover regions between the radiative and nonradiative ones.

region B with strong intersite interaction K survives the thermal fluctuations. However, the spontaneous emission is possible both near $n_e=0$ and $n_e=1$, and the threshold intensity $I_{\rm th}$ defined in Sec. III is very large. Therefore we conclude that in order to obtain the switching phenomenon with reasonable pumping intensity, one should keep the temperature low compared with the lattice relaxation energy.

The dynamics in the case of finite temperature will be discussed in detail in a forthcoming paper taking also the time-resolved emission spectra, fluctuation effects, and applications to the real system into account.

B. Comparison with experimental results on PDA

As an example of the application of our theoretical model, we discuss the photoisomerization (A-B transition) of various polydiacetylenes (PDA's). There are many kinds of PDA crystals according to their side chains. PDA's are, however, rather distinctly classified into two type, i.e., A (blue) form and B (red) form. The following experimental facts have been obtained.[5–11,19,20]

(1) The A form is the low-temperature phase while the B form is the high-temperature phase. There is a first-order phase transition at T_c ($\sim$330 K) with the hysteresis. There are some PDA's whose A-B transition is accompanied by the order-disorder transition of the hydrogen bonding between the side groups.

(2) The absorption energy due to the ^1B_u exciton is 1.9 eV in the A form and 2.3 eV in the B form, respectively. The emission of light is observed only in the B form with the Stokes shift 0.4 eV.

(3) Some PDA's, e.g., TCDU, ETCD, and PDA-(10,8), -(12,8), and -(14,8), show the photoinduced isomerization from A to B form not from B to A form. The following facts have been revealed. (3a) The photoinduced absorption is observed in the A form with the lifetime $\tau\sim 50$ μs. (3b) The photoinduced ESR signal is found indicating the triplet excited states. (3c) The conversion efficiency ϕ_{AB} from A to B form as a function of the energy of the incident light of PDA-(12,8) rises, not at the energy of the ^1B_u exciton ($\sim$1.8 eV) which contributes the absorption, but at the energy of the ^1A_g exciton. (3d) The conversion efficiency ϕ_{AB} is a strongly nonlinear function of the intensity I_0 of the incident light with the duration time t_0 being fixed. Tokura *et al.* found the relation $\phi_{AB}\propto I_0^3$ while the recent investigations have revealed the thresholdlike behavior around an intensity $I_{\rm th}$. (3e) The conversion efficiency ϕ_{AB} from A to B form by the two laser pulses depends on the time interval of the two pulses.

It should be noted that our model is too simple to describe the photoinduced A-B transition in PDA's in detail. The effects of the triplet exciton, the hydrogen bonding of the side groups, etc. are neglected, and the discussion below is of semiquantitative and rather phenomenological nature. Therefore we determine the parameters $E_{\rm FC}$, S, and K tentatively as follows. We regard the B form as the state with $n_e=0$. From (2) above we have the following equalities:

$$E_{\rm FC}=2.3\ \text{eV}\ , \tag{4.4a}$$

$$\frac{S}{1-K}-E_{\rm FC}=1.9\ \text{eV}\ , \tag{4.4b}$$

$$S=0.4\ \text{eV}\ . \tag{4.4c}$$

From Eqs. (4.4) we obtain

$$\tilde{S}=S/E_{\rm FC}=0.17\ , \tag{4.5a}$$

$$K=0.91\ . \tag{4.5b}$$

The detailed values of $\tilde{S}$ and K have little meaning when one considers the roughness of our model, but it can be said that the PDA's are characterized by the strong coupling between the local structure changes and the nonlinearity derived from it, which is also verified experimentally as has been listed in (3a), (3d), and (3e). The point $(K,\tilde{S})$ in Eqs. (4.5) belongs to the B region in Fig. 3. But is would be better to make it assign to the D region from the experimental fact (2). In practice, the photoinduced structure change would be difficult when the function $u(n_e)$ is of the form like Fig. 6, region B, because the "restoring force" against the optical pumping is much stronger in Fig. 6, region B than in Fig. 6, region D. These considerations are consistent with the fact that the photoinduced structure change is observed only from the A to B form not form B to A. At room temperature ($T=300$ K), the reduced temperature $\bar{T}$ is 0.065, and α is about 1400. Therefore we can apply the consideration in Sec. IV to the photoinduced dynamics of PDA's, but the detailed discussion including the comparison with experiments is left for future publications. The exchange J and the field h defined in this section are obtained as follows:

$$J=3.8\ \text{eV}\ , \tag{4.6a}$$

$$h=-0.2\ \text{eV}\ . \tag{4.6b}$$

The value of h is doubtful. Experimentally, the A form has lower energy. We consider that this discrepancy is perhaps due to the contributions of the side groups to the free energy which are not taken into account in our model, and h should be interpreted as a temperature-dependent quantity which changes sign at the A-B transition temperature. The relative role of the thermal and photoinduced nucleation processes depend on the temperature through both the activation factor and h. Therefore systematic studies of the temperature dependence of the photoinduced dynamics are strongly desired, and these problems are left for future investigations.

In conclusion we have proposed a simple model to discuss the photoinduced structure changes from a unified point of view. We have classified photoinduced dynamics in the K-$\tilde{S}$ plane, and discussed the threshold behavior, relaxation time, and the spontaneous emission stressing their temperature dependence in the mean-field approximation. The respective roles of thermal and optical transitions are discussed. These considerations are applied to the A-B transition of polydiacetylenes and their collective nature has been pointed out. We hope that our model can be one of the guiding models in searching for and designing the new materials in terms of the information

storage. Our model can be extended to the glassy systems, which have many metastable states, and the relationship to the spin-glass model[21] and neutral network model[22] will be discussed elsewhere.

ACKNOWLEDGMENTS

The authors acknowledge Professor T. Koda, Professor E. Hanamura, Professor Y. Tokura, Dr. T. Kanetake, Dr. K. Ishikawa, and T. Nagai for discussions. This work has been partially supported by the Scientific Research Grant-in-Aid from the Ministry of Education, Science and Culture of Japan.

APPENDIX A: THE BOUNDARY BETWEEN SWITCHING AND NONSWITCHING REGIONS

The mean-field equation is

$$\langle M\rangle=\tfrac{1}{2}\tanh\left[\frac{1}{2k_BT}(h+J\langle M\rangle)\right], \tag{A1}$$

where J, h, and $\langle M\rangle$ are given in the text.

Equation (A1) is rewritten as follows:

$$x=G(x)=\left[\exp\left[\frac{1}{a}(b-x)\right]+1\right]^{-1}, \tag{A2}$$

with

$$x=\langle M\rangle+\tfrac{1}{2}, \tag{A3a}$$

$$a=\frac{k_BT}{J}, \tag{A3b}$$

$$b=\tfrac{1}{2}-\frac{h}{J}. \tag{A3c}$$

The boundaries which separate the one- and three-solution regions are obtained by the condition that the tangents of $y=G(x)$ with the slope 1 coincide with $y=x$. The derivative of $G(x)$ with respect to x is

$$\frac{dG(x)}{dx}=\frac{1}{a}\exp\left[\frac{1}{a}(b-x)\right]\left[\exp\left[\frac{1}{a}(b-x)\right]+1\right]^{-2}. \tag{A4}$$

Equating $dG(x_0^{\pm})/dx$ with unity, we obtain

$$x_0^{\pm}=b-a\ln\left[\frac{1-2a\pm\sqrt{1-4a}}{2a}\right], \tag{A5}$$

for $a<\frac{1}{4}$. Equation (A2) has only one solution for $a>\frac{1}{4}$. Putting $x_0^{\pm}$ in Eq. (A5) into Eq. (A2), we obtain the two boundaries within which (A2) has three solutions:

$$x_0^{\pm}=G(x_0^{\pm}). \tag{A6}$$

Equation (A6) is solved for b as follows:

$$b=f_{\pm}(a)\equiv\frac{2a}{1\pm\sqrt{1-4a}}+a\ln\left[\frac{1-2a\pm\sqrt{1-4a}}{2a}\right]. \tag{A7}$$

Consequently, the condition for the existence of three solutions is

$$f_+(k_BT/J)<\tfrac{1}{2}-\frac{h}{J}<f_-(k_BT/J), \tag{A8}$$

which is rewritten as

$$\Theta_-(K)<\tilde{S}<\Theta_+(K), \tag{A9}$$

for $4\tilde{T}/(1+4\tilde{T})<K<1$ with $\tilde{T}\equiv k_BT/S$. The functions $\Theta_+(K)$ and $\Theta_-(K)$ are given by

$$\Theta_{\pm}(K)=\left[\frac{1}{2}+\frac{K}{1-K}f_{\pm}\left[\frac{1-K}{K}\tilde{T}\right]\right]^{-1}, \tag{A10}$$

with the functions $f_+(x)$ and $f_-(x)$ being given in Eq. (A7). Hereafter, we call Eq. (A9) the switching condition and the region which satisfies it the switching region. Outside the switching region, we have only one solution. The two functions $\Theta_+(K)$ and $\Theta_-(K)$ meet at

$$(K_1,\tilde{S}_1)=\left[\frac{4\tilde{T}}{1+4\tilde{T}},\frac{2}{1+4\tilde{T}}\right], \tag{A11}$$

which is the so-called critical point. As the temperature $\tilde{T}$ goes to zero, $\Theta_+(K)$ approaches 2, and $\Theta_-(K)$ approaches $2(1-K)/(1+K)$. These are the zero-temperature boundaries. The line where the absolute stability and metastability are exchanged is $\tilde{S}=2(1-K)$ for all temperatures because of the symmetry between g and e states on that line and the critical point (A11) lies on it.

APPENDIX B: OPTICAL TRANSITION PROBABILITIES

We treat the displacement Q as the classical coordinate, and the optical transition is vertical with respect to Q (Franck-Condon principle).[15] Therefore the transition probabilities between the upper level a and the lower level b for each Q are given as follows:

$$P_{a\to b}^{\text{down}}(Q)=\frac{1}{\tau_r}[1+N_B(E_a(Q)-E_b(Q))]F(Q), \tag{B1a}$$

$$P_{b\to a}^{\text{up}}(Q)=\frac{1}{\tau_r}N_B(E_a(Q)-E_b(Q))F(Q), \tag{B1b}$$

where τ_r is the lifetime for the spontaneous emission for $Q=0$, and $N_B(x)$ is the Bose distribution function which represents the thermal occupation of the photon:

$$N_B(x)=\left[\exp\left[\frac{x}{k_BT}\right]-1\right]^{-1}. \tag{B2}$$

The function $F(Q)$ is given by

$$F(Q)=\left|\frac{E_a(Q)-E_b(Q)}{E_{FC}}\right|^3\times\left|\frac{\langle\Psi_a(\mathbf{r},Q)|\mathbf{r}|\Psi_b(\mathbf{r},Q)\rangle}{\langle\Psi_a(\mathbf{r},Q=0)|\mathbf{r}|\Psi_b(\mathbf{r},Q=0)\rangle}\right|^2, \tag{B3}$$

where $\Psi_a(\mathbf{r},Q)$ [$\Psi_b(\mathbf{r},Q)$] is the electronic wave function of the upper level a (lower level b) for the displacement Q. Note that $F(Q=0)$ is unity because

$$E_a(Q=0)-E_b(Q=0)=E_e(Q=0)-E_g(Q=0)=E_{FC}\ , \tag{B4}$$

for $Q=0$ in Fig. 1. The form of the function $F(Q)$ depends upon the Q dependence of the matrix element of the transition dipole moment, but it should cancel out the divergence of the Bose factor at $E_a(Q)=E_b(Q)$. Strictly speaking, the off-diagonal element between a and b states mixes the two branches near the crossing point. But we avoid this complexity by simply assuming $F(Q)$ vanishes at the crossing point because the thermal transitions dominate in this region as is discussed in the text.

Applying the above argument to the energy diagram in Fig. 1, the indices a and b correspond to e state (g state) and g state (e state), respectively, for $Q<E_{FC}/\sqrt{S}$ ($Q>E_{FC}/\sqrt{S}$). The energy difference for each Q is given by

$$E_a(Q)-E_b(Q)=E_e(Q)-E_g(Q)$$
$$=E_{FC}-\sqrt{S}Q \quad \text{for } Q<E_{FC}/\sqrt{S}\ , \tag{B5a}$$

$$E_a(Q)-E_b(Q)=E_g(Q)-E_e(Q)$$
$$=\sqrt{S}Q-E_{FC} \quad \text{for } Q>E_{FC}/\sqrt{S}\ . \tag{B5b}$$

At has been discussed in Sec. II, we assume that the thermal equilibrium within the parabola is attained at once and the distribution of Q is given in Eqs. (2.3). Thus we obtain the expression of the optical transition probabilities as Eqs. (2.19).

[1]G. Smets, Adv. Polym. Sci. **50**, 17 (1983).

[2]W. E. Moerner, J. Mol. Electron. **1**, 55 (1985).

[3]H. Bässler, H. Sixl, and V. Enkelmann, in *Polydiacetylenes,* Vol. 63 of *Advances in Polymer Science,* edited by H.-J. Cantow (Springer-Verylag, Berlin, 1984).

[4]M. Hasegawa, Chem. Rev. **83**, 507 (1983).

[5]Z. Iqbal, R. R. Chance, and R. H. Baughman, J. Chem. Phys. **66**, 5520 (1977).

[6]R. R. Chance, R. H. Baughman, H. Muller, and C. J. Eckhardt, J. Chem. Phys. **67**, 3616 (1977).

[7]Y. Tokura, T. Kanetake, K. Ishikawa, and T. Koda, Synth. Met. **18**, 407 (1987).

[8]T. Kanetake, Y. Tokura, and T. Koda, Solid State Commun. **56**, 803 (1985).

[9]T. Kanetake, Y. Tokura, T. Koda, T. Kotaka, and H. Ohnuma, J. Phys. Soc. Jpn. **54**, 4014 (1985).

[10]Y. Tokura, K. Ishikawa, T. Kanetake, and T. Koda, Phys. Rev. B **36**, 2913 (1987).

[11]T. Kanetake, K. Ishikawa, T. Koda, Y. Tokura, and K. Takeda, Appl. Phys. Lett. **51**, 1957 (1987).

[12]E. Hanamura and N. Nagaosa, Solid State Commun. **62**, 5 (1987).

[13]E. Hanamura and N. Nagaosa, J. Phys. Soc. Jpn. **56**, 2080 (1987).

[14]T. Nagai, N. Nagaosa, and E. Hanamura, J. Lumin. **38**, 314 (1987).

[15]See, e.g., M. Ueta, H. Kanzaki, K. Kobayashi, Y. Toyozawa, and E. Hanamura, *Excitonic Processes in Solids* (Springer-Verlag, Berlin, 1986), Chap. 4.

[16]J. D. Gunton and M. Droz, *Introduction to the Theory of Metastable and Unstable States,* Vol. 183 of *Lecture Notes in Physics* (Springer-Verlag, Berlin, 1983).

[17]Only under low temperature, the relative locations of the minima of $U(n_e)$ to n_L and n_U are a good measure for the quantitative difference of the optical transition in the relaxation process. The minima of the potential $U(n_e)$ coincide, respectively, with n_L and n_U on the lines described as

$$\tilde{S}=\Phi_+(K)=\frac{\exp(1/2\tilde{T})+1}{\exp(1/2\tilde{T})+(1-K)^{-1}}\ ,$$

$$\tilde{S}=\Phi_-(K)=\frac{1-K}{K}\left[\exp\left[-\frac{1}{2\tilde{T}}\right]+1\right]\ ,$$

which are derived by inserting n_L and n_U into the mean-field equation [e.g., Eq. (A1)]. In the case of high temperature, however, these criteria lose their mean because the crossover between the radiative and nonradiative regions becomes conspicuous and veils the above criteria.

[18]Strictly speaking, there exist more very small regions in Figs. 7(a) and 7(b). However, they are very narrow and cannot be detected because of the thermal uncertainty so that we do not discuss them.

[19]T. Kanetake, K. Ishikawa, and T. Koda (private communications).

[20]K. Fukagai *et al.* (unpublished).

[21]S. F. Edwards and P. W. Anderson, J. Phys. F **5**, 965 (1975).

[22]D. J. Amit, H. Gutfreund, and H. Sompolinsky, Ann. Phys. (N.Y.) **173**, 30 (1987).